Journal on Oncology

www.journalononcology.org

Research Article

Open Access, Volume 4

Synthesis, Characterization, and Anticancer Activity Studies of the Novel Pyridinyl Zn (II) and Ni (II) Metal Complexes

Yang Yan-Ting; Hu Bai-Quan; Luo Mei*

Hefei University of Technology, School of Chemistry and Chemical Engineering, Hefei 230000, China.

Abstract

Four novel organometallic complexes were obtained via direct reactions of 2-amino-3-formaldehyde pyridine and 3,4-diaminopyridine with transition metal zinc salts ($Zn(CH_3COO)_2 \cdot 2H_2O$ and $Zn(NO_3)_2 \cdot 2H_2O$) and nickel salts ($Ni(CH_3COO)_2 \cdot 4H_2O$ and $Ni(NO_3)_2 \cdot 6H_2O$), respectively, under one-pot conditions, i.e., $[C_{16}H_{22}N_4NiO_8]$ (I), $[C_{14}H_{20}N_6O_4Zn]$ (II), $[C_{10}H_{20}N_{10}NiO_{14}]$ (III), and $[C_{10}H_{20}N_{10}O_{14}Zn]$ (IV). The structures of the complexes were characterized via X-ray diffraction (XRD), Infrared Spectroscopy (FT–IR), Ultraviolet–Visible Spectroscopy (UV–vis), and Electrospray ionization Mass Spectrometry (ESI–MS), and the inhibition of the complexes against cancer cell lines (lung cancer A549, liver cancer SMMC-7721, breast cancer MDA-MB-231, and colon cancer SW480) was tested via the MTS method. These results show that complex I has a better inhibitory effect on SMMC-7721 and SW480 cells than does complex II alone and that complex II has a better inhibitory effect on the SW480 cancer cell line.

Keywords: 2-Amino-3-formylpyridine; 3,4-diaminopyridine; One-pot method; Organometallic complex; Biological activity.

Introduction

Cancer is regarded as one of the «three major killers» threatening human health, and for many years, countless researchers have devoted themselves to researching anticancer agents in the hope of improving the survival rates of cancer patients. In 1978, cisplatin drugs were successfully used in the clinic, which was epochal in the history of the fight against cancer in humans [1]. Platinum drugs are still important means of cancer treatment, but platinum anticancer drugs also have several limitations, such as strong toxic side effects and poor selectivity. In this context, researchers have begun to turn their attention to the field of transition metal-organic complexes. Metal-organic complexes have the advantages of structural diversity and functional design ability and have a wide range of applications in fields such as catalysis [2], sensing [3], and medicinal chemistry [4]. The structural properties and biological properties of ligands and metal ions are among the key factors determining the applied functions of complexes [5,6], and the geometries, thermal stabilities, solubilities, and chemical properties of complexes synthesized with different ligands and metal ions are very different. Therefore, a crucial step in the synthesis of complexes is the selection of suitable ligands and metal ions [7]. The unique structural and pharmacological features of heterocyclic compounds are important for the discovery and preparation of novel drugs. According to a survey, nitrogen-containing heterocyclic drugs account for more than three-quarters of the 164 drug molecules approved by the U.S. Food and Drug Administration during 2015-2020 [8-10], among which the most analysed drugs are pyridine analogues, which have a wide range of biological activities, such as antiviral, antibacterial,

Manuscript Information: *Received: Jul 19, 2024; Accepted: Aug 14, 2024; Published: Aug 21, 2024*

Correspondance: *Luo Mei, Hefei University of Technology, School of Chemistry and Chemical Engineering, Hefei 230000, China.*

Email: luomei@pku.edu.cn

Citation: *Yan-Ting Y, Bai-Quan H, Mei L. Synthesis, Characterization, and Anticancer Activity Studies of the Novel Pyridinyl Zn (II) and Ni (II) Metal Complexes. J Oncology. 2024; 4(2): 1141.*

and anticancer activities [11]. In addition, pyridine analogues are an important class of multifunctional ligands, and their special heterocyclic structure allows them to coordinate with a variety of metals to form stable complexes. Therefore, 2-amino-3-formaldehyde pyridine and 3,4-diaminopyridine were chosen as ligands in this work, and the coordination function of the ligands with metals was further enhanced because each ligand contains several excellent electron-donor sites, i.e., the N atoms of the pyridine ring, the N atoms of the amino group, and the O atoms of the aldehyde group [12,13]. Compared with other metals, transition metals, as essential trace elements, have the advantages of low toxicity, easy availability of raw materials and low experimental costs. Zinc and nickel are indispensable trace elements for human development and are involved in various biological functions of the human body, such as biological enzyme activity, growth and tissue regeneration, and immune response [14-16]. A variety of zinc and nickel metal complexes have been shown to have excellent biological activities and can be used to treat a variety of diseases worldwide [17,18].

These complexes are synthesized via a one-pot method, which is easy to perform, inexpensive, simple and efficient [19,20]. In this work, four novel metal-organic complexes were reported, and the structures of the complexes were characterized via XRD, FT-IR, UV-vis and ESI-MS. The anticancer activities of the four complexes against four cancer cell lines, namely, A549, SMMC-7721, MDA-MB-231, and SW480, were tested via the MTS method to preliminarily determine whether the complexes have anticancer potential.

Experimental

Materials and instruments

Reagents such as 2-amino-3-formaldehyde pyridine, 3,4-diaminopyridine, $Ni(CH_3COO)_2{\cdot}4H_2O$, $Zn(CH_3COO)_2{\cdot}2H_2O$, $Ni(NO_3)_2{\cdot}6H_2O$, $Zn(NO_3)_2{\cdot}2H_2O$, CH_3CH_2OH, CH_3OH, and DMF were analytically pure without any purification operation. The crystal structures of complexes (I)-(IV) were obtained on a Bruker D8 Venture diffractometer. Infrared spectra were recorded on a Mattson Galaxy Series FTIR 3000 spectrometer; peaks are given in cm^{-1}. ESI–MS data were measured on a Vanquish Q Exactive Plus liquid Chromatography-quadrupole electrostatic field orbit trap mass spectrometer. The melting points of the complex crystals were measured by an X-4S digital micro melting point apparatus.

X-ray structure

Crystallographic data for complexes (I)-(IV) were collected on a Bruker D8 Venture diffractometer using Ga Ka (λ=1.34139 Å) radiation. Using OLEX2 [21], the structure was solved with the SHELXT [22] structure solution program via intrinsic phasing and refined with the SHELXL-2018/3 [23] refinement package via least squares minimization. In complexes (I)-(IV), all non-H atoms were refined with anisotropic thermal parameters.

Cytotoxicity assay

In this study, the MTS method was used to test the inhibitory effects of complexes (I)-(IV) on four cancer cell lines: lung cancer A549, liver cancer SMMC-7221, breast cancer MDA-MB-231, and colon cancer SW480. The experiments were carried out by using 10% foetal bovine serum culture medium to formulate individual cell suspensions and inoculate them into 96-well plates. Then, the complex solution dissolved with DMSO at a 100 μM concentration was added for primary screening, and three replicate wells were set for each complex. After 48 h of incubation at 37°C, 20 μl of MTS solution was added to each well, and the incubation was continued for 2-4 h. The final calculation of the cell inhibition rate was performed by determining the light absorption value of each pore.

General steps for the synthesis of complexes

Complexes (I)-(IV) were synthesized in a similar way (Figure 1). The ligands and metal salts were heated and refluxed in anhydrous ethanol or anhydrous methanol at a specific ratio for 24-48 h and then thermally filtered. The filtrate was placed in a beaker and sealed with a sealing film, and small holes were created in the sealing film with a fine needle to cultivate the crystal structure suitable for X-ray diffraction in a suitable solvent. The obtained crystals were washed three times with hexane or petroleum ether and then vacuum dried for 30 min to obtain the expected product. The cultivation of complex crystals is essentially a process of recrystallization from a saturated solution. Generally, the growth of crystals is related to two external factors, namely, the solvent and temperature, and the structure of cultured crystals may be very different depending on the solvent. The most common method of growing complex crystals in the laboratory is the solution method, i.e., the solution is gradually saturated by evaporation of the solvent in the solution, and the target crystals are eventually obtained. If the desired crystals cannot be obtained, one can consider changing to another solvent or changing the temperature, such as by trying low-temperature precipitation in a refrigerator. In this experiment, we used the above method to obtain a crystal structure suitable for XRD analysis.

Synthesis of complex (I)

The ligand 2-amino-3-formaldehyde pyridine (0.2456 g, 2 mmol) was weighed and dissolved in 25 mL of anhydrous methanol, and then, $Ni(CH_3COO)_2{\cdot}4H_2O$ (0.2492 g, 1 mmol) was added to the above mixture and stirred until it was dissolved. The mixture was subsequently transferred to a 100 mL round-bottom flask, stirred and refluxed for 24 h at 80°C. The mixture was subjected to hot filtration, the resulting filtrate was allowed to evaporate naturally at room temperature, and light green crystals suitable for X-ray single-crystal analysis were eventually obtained. The mass was 0.2608 g, the yield was 57.06%, and the m.p. was 89-91 ℃. IR(KBr), υ, cm^{-1}: 3447, 3336(N-H); 1667(C=O); 1570, 1455(C=C); 1408 (C=N); 1360, 1272 (C-N); 1218, 1140 (C-O-C); 3200-3030, 910(O-H); 671(Ni-O); 546(Ni-N). ESI-MS, m/z: 456.07 $[M-H]^+$.

Synthesis of complex (II)

The ligand 3,4-diaminopyridine (0.2199 g, 2 mmol) was weighed and dissolved in 40 mL of anhydrous methanol. Then, 2-aminopyrimidine (0.0968 g, 1 mmol) was added, and the mixture was stirred until it was dissolved. $Zn(CH_3COO)_2{\cdot}2H_2O$ (0.2245 g, 1 mmol) was added to the above mixture, which was then stirred and refluxed for 24 h at 80°C. After hot filtration, the filtrate volatilised naturally in air, and yellow granular crystals eventually precipitated. The dried mass was 0.2048 g, the yield was 51.07%, and the m.p. was 183-185°C. IR (KBr), υ, cm^{-1}: 3400, 3340(N-

H); 1525, 1450 (C=C); 1400(C=N); 1330, 1275(CN); 1600(C=O); 1200, 1068(C-O-C); 678(Ni-O); 595, 545(Ni-N). ESI-MS, m/z: 402.91[M+H]$^+$.

Synthesis of complex (III)

Similar to the above experimental method, first, the ligand 3,4-diaminopyridine (0.2195 g, 2 mmol) was dissolved in 50 mL of anhydrous methanol, heated and stirred until completely dissolved. Second, 2-aminopyrimidine (0.0941 g, 1 mmol) was added, and the mixture was stirred until it was dissolved. Last, $Ni(NO_3)_2{\cdot}6H_2O$ (1.7973 g, 6 mmol) was added, the reaction temperature was controlled at 90°C, and the mixture was stirred at reflux for 48 h and then hot-filtered. The filtrate was volatilised naturally at room temperature, and green lumpy crystals eventually precipitated from the mother liquor. The mass was 0.3400 g, the yield was 60.38%, and the m.p. was 209-212°C. IR (KBr), υ, cm^{-1}: 3420, 3355(N-H); 3115, 2965, 3090(C-H); 3250(O-H); 1650, 1605, 1570(C=C); 1510(C=N); 1320, 1185(C-N); 1385(N-O); 610(Zn-O); 511(Zn-N). ESI-MS, m/z: 562.36[M-H]$^+$.

Synthesis of complexes (IV)

3,4-diaminopyridine (0.2179 g, 2 mmol) and $Zn(NO_3)_2{\cdot}2H_2O$ (0.2204 g, 1 mmol) were dissolved in 40 mL of anhydrous methanol at 2:1, refluxed at 80°C for 24 h and then filtered while it was still hot. The filtrate was volatilised naturally at room temperature, and after some time, a yellow oily solid appeared, which was recrystallised with a mixture of DMF (12 mL) and anhydrous methanol (6 mL) for recrystallisation. After four months, yellow–brown crystals precipitated. The mass was 0.4147 g, the yield was 73%, and the m.p. was 122-125℃. IR (KBr), υ, cm^{-1}: 3418, 3345 (N-H); 3148, 3091, 3003 (C-H); 3238 (O-H); 1645, 1610, 1568 (C=C); 1510 (C=N); 1295, 1172 (C-N); 1386 (N-O); 654, 602 (Zn-O); 528 (Zn-N). ESI-MS, m/z: 570.74[M+H]$^+$.

Results and discussion

X-ray diffraction analysis

The crystal structures of complexes (I)-(IV) are shown in Figure 1. Complexes (I)-(IV) are monoclinic crystal systems and contain only one metal centre. The space groups are denoted as $P2_1/c$, $P2_1/n$, $P2_1/n$, and $P2_1/c$. The crystal data and refinement parameters of the complexes are shown in Table 1, and some hydrogen bonding data are shown in Table 2.

The complex (I) crystal is composed of one Ni^{2+}, two ligand molecules, two water molecules, and two acetate ions. The central ion Ni^{2+} forms an octahedral configuration with N atoms on the two-ligand pyridine rings, O atoms on the two water molecules, and O atoms on the two acetates, with N(1)-Ni(1)-N(1A), O(2)-Ni(1)-O(2A), and O(4)-Ni(1)-O(1A) bonding angles of 180°, respectively. The molecules are interconnected by hydrogen bonding along the b-axis direction overlapping each other and then along the c-axis direction connecting to form a chain, finally forming a lamellar structure.

The cell of complex (III) contains two complex cations, two $[Ni(NO_3)_4]^{2-}$ ions, two water molecules, and two free nitrate ions. The central atom Ni^{2+} adopts a six-coordinate configuration, constituting an octahedral configuration with the axial position occupied by O(O1,O4) on the two nitrate ions, whereas the N atoms (N1,N4) of the two ligand molecules and the O atoms (O7,O8) in the two water molecules jointly form the equatorial plane, i.e., O(7)-Ni(1)-N(1), O(7)-Ni(1)-N(4), O(8)- Ni(1)-N(1), and O(8)-Ni(1)-N(4) bond angles sum to 360°. The major bond lengths of the complex (III) crystals are $d_{Ni(1)-O(1)}$ = 2.0731(15)Å, $d_{Ni(1)-O(4)}$ = 2.0818(15)Å, dNi(1)-O(7) = 2.0505(15)Å, dNi(1)-O(8) = 2.0506(15) Å, dNi(1)-N(1) = 2.1491(16) Å, and dNi(1)-N(4) = 2.1502(17) Å. The ligand and water molecules separated by C-H…O, N-H…O, O-H…O, and O-H…O hydrogen bonding interactions have a three-dimensional mesh stacking structure.

Complex (IV) is structurally similar to complex (III), but complex (IV) is centred on Zn^{2+} with a coordination number of six. Since none of the three bond angles, N(1)-Zn(1)-N(4), O(3)-Zn(1)-O(4), or O(13)-Zn(1)-O(14), is 180° and the axial lengths are unequal, it is not symmetric and hence is not an octahedral configuration. The molecules are connected in the b-axis direction by C-H…O, N-H…O, and O-H…O hydrogen bonds to form a regular mesh structure.

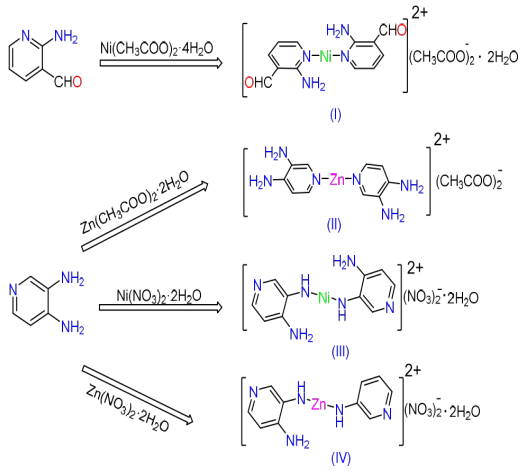

Figure 1: Synthesis routes of complexes (I)-(IV).

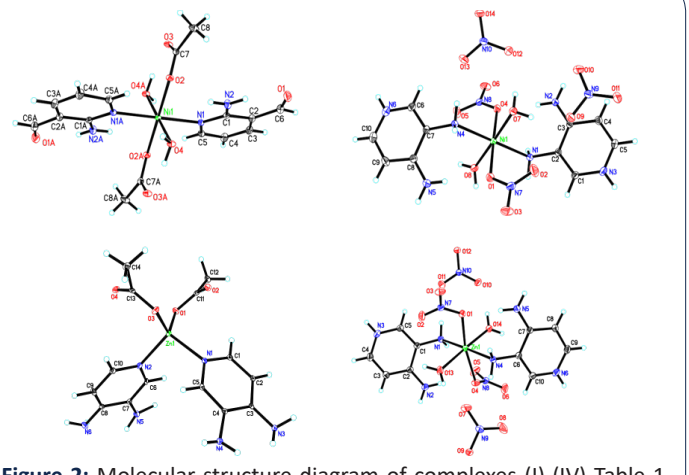

Figure 2: Molecular structure diagram of complexes (I)-(IV) Table 1 Crystallographic parameters and crystallographic data for complexes (I)-(IV).

Table 1: Crystallographic parameters and crystallographic data for complexes (I)-(IV).

Complex	I	II	III	IV
Empirical formula	C16 H22 N4 Ni O8	C14 H20 N6 O4 Zn	C10 H20 N10 Ni O14	C10 H20 N10 O14 Zn
Formula weight	457.08	401.73	563.07	569.73
Temperature	100.0 K	100(2) K	200(1) K	200(2) K
Wavelength	1.34139	1.34139	1.34139	1.34139
Crystal system	Monoclinic	Monoclinic	Monoclinic	Monoclinic
Space group	$P2_1/c$	$P2_1/n$	$P2_1/n$	$P2_1/c$
a/Å	9.1327(18)	10.7302(7)	11.0904(5)	7.1800(2)
b/Å	12.479(2)	10.7786(7)	14.5935(6)	27.6689(9)
c/Å	8.8488(18)	14.5358(9)	13.7304(6)	11.0795(4))
α/°	90	90	90	90
β/°	104.414(10)	95.295(3)	110.341(2)	107.5450(10)
γ/°	90	90	90	90
Volume	976.8(3)	1673.99(19)	2083.66(16)	2098.69(12)
Z	2	4	4	4
Dcalcd g/cm^3	1.554	1.594	1.795	1.803
μ (mm^{-1})	5.732	1.537	5.649	1.635
F(000)	476.0	832.0	1160	1168
2θ range (°)	10.666-144.546	8.9-144.554	7.726-129.674	2.779-72.402
Reflections collected	14150	32153	34390	57147
Independent reflections	2914	4984	5327	3290
Final R indices [I >= 2σ(I)]	R1=0.0554, wR2=0.1260	R1=0.0642, wR2=0.1361	R1=0.0430, wR2=0.1123	R1 = 0.0300, wR2 = 0.0808
Final R indices [all data]	R1=0.0745, wR2=0.1335	R1=0.0729, wR2=0.1388	R1=0.0529, wR2=0.1178	R1 = 0.0374, wR2 = 0.0839
Residuals (e.Å3)	1.07/-0.76	0.70/-0.68	1.01/-0.69	0.397/-0.344

Table 2: Partial hydrogen bond data for complexes (I)-(IV).

D-H···A	d(D-H)/Å	d(H···A)/Å	d(D···A)/Å	∠(DHA)/°
Complex I				
N(2)-H(2A)...O(2)	0.88	2.15	2.830(3)	133.1
O(4)-H(4A)...O(3)#1	0.87	1.87	2.666(2)	150.5
Complex II				
C(6)-H(6)...O(3)#1	0.95	2.29	3.130(3)	147.1
N(4)-H(4A)...O(4)#3	0.88	2.15	3.000(3)	160.3
Complex III				
C(1)-H(1)...O(12)#1	0.95	2.55	3.186(3)	124.6
N(2)-H(2B)...O(4)	0.88	2.06	2.897(2)	158.3
N(6)-H(6A)...O(9)#3	0.88	2.00	2.868(2)	171.0
O(7)-H(7A)...O(12)	0.85	1.97	2.758(2)	153.4
Complex IV				
C(4)-H(4)...O(6)#1	0.95	2.31	3.0380(17)	133.0
N(1)-H(1B)...O(3)#5	0.91	2.43	3.0298(13)	123.4
N(5)-H(5B)...O(1)	0.88	2.16	2.9601(14)	151.7
O(13)-H(13B)...O(7)	0.87	1.94	2.7589(16)	155.4

Infrared absorption spectra of complexes (I)-(IV)

Figure 3 shows all the absorption peaks of the IR spectra of complexes (I)-(IV) measured between 400 and 4000 cm^{-1}. The ligands of complexes (I)-(IV) are aminopyridine compounds, so the double absorption peaks of the telescopic vibration of the N–H bond of the primary amine can be observed in the range of 3500-3300 cm^{-1} (3447 cm^{-1} and 3336 cm^{-1} for complex I; 3400 cm^{-1} and 3340 cm^{-1} for complex II; 3420 cm^{-1} and 3335 cm^{-1} for complex III; 3418 cm^{-1} and 3335 cm^{-1} for complex IV; 3418 cm^{-1} and 3335 cm^{-1} for complex IV; and 3418 cm^{-1} and 3335 cm^{-1} for complex IV).

The characteristic absorption peaks attributed to the -C–N bond at 1360-1250 cm^{-1} (complex I: 1360 cm^{-1}; complex II: 1330 cm^{-1}; complex III: 1320 cm^{-1}; and complex IV: 1295 cm^{-1}) and 1280-11180 cm^{-1} (complex I: 1272 cm^{-1}; complex II: 1275 cm^{-1}; complex III: 1185 cm^{-1}; and complex IV: 1172 cm^{-1}) prove that the amino group is directly connected to the benzene ring. The pyridine ring is similar in structure to the benzene ring, with only one carbon atom replaced by a nitrogen atom. Thus, the infrared absorption spectra have only slight differences. The -C–H stretching vibration of the pyridine ring is the same as that of the benzene ring, with three weak absorption peaks in the range of 3100-3000 cm^{-1}, and the corresponding absorption peaks from the infrared spectrograms of complexes (I)-(IV) correspond to these peaks [24]. The C=C and C=N bonds on the pyridine ring have strong absorption peaks in the range of 1683-1410 cm^{-1} [25].

Generally, the vibrational frequency of the aldehyde carbonyl group is near 1725 cm^{-1}, but the vibrational frequency of the -C=O bond is shifted in the direction of low wavenumbers due to the conjugation of the aldehyde group with the aromatic ring, which results in a reduction in the electron cloud density on the carbonyl carbon atom; thus, the -C=O telescopic vibration of complex I is in the vicinity of 1667 cm^{-1}. The peaks of the -O–H stretching vibration were observed in the range of 3500-3000 cm^{-1} for all the synthesised complexes, with the exception of complex II, which is attributed to the effect of intermolecular hydrogen bonding of the complexes, which changes the vibrational frequency of -O–. The vibrational frequency of the ester carbonyl group is generally near 1735 cm^{-1}, and the absorption peak is a strong broad peak. Owing to the formation of intermolecular hydrogen bonds between the carbonyl oxygen atoms of complexes I and II and the amino hydrogen atoms on other molecules, which resulted in a reduction in the force constant of the -C=O bond, the telescopic vibration absorption frequency moved to lower wavelengths at 1628 cm^{-1} and 1600 cm^{-1}, respectively, and the spectral band became broader and the peak intensity increased. Both complexes III and IV have a strong absorption peak near 1385 cm^{-1}, which is caused by the stretching vibration of the -N–O bond in nitrate, and this peak represents strong evidence of the existence of nitrate. In addition to the above characteristic peaks, we can also observe some weak absorption peaks in the ranges of 650-600 cm^{-1} and 600-500 cm^{-1} for the stretching vibration peaks of the M–N and M–O bonds, which also indicates that coordination between the metal and the ligand occurs [26].

UV-Vis spectra of complexes (I)-(IV)

The UV spectra of complexes (I)-(IV) in anhydrous ethanol are shown in Figure 4. The absorption peak of complex I at 260 nm is attributed to the n→π* jump on the ligand C=O. Since there is no significant displacement of the absorption peak after coordination, C=O in the ligand is not involved in the coordination, which is consistent with the results of the crystal structure analysis via X single-crystal diffraction [27]. The ligands of complexes I-IV contain an aromatic ring to which an n-electron cochromophore, NH_2, is attached, leading to an n-π conjugation, which causes a redshift of the E and B bands of the aromatic ring, and the π→π* leaps on the conjugated alkene bond of the pyridine ring near 232 nm as well as the π→π* leap on the closed alkene bond of the pyridine ring near 305 nm. Notably, complex I has a broad absorption peak at 350 nm with a d-d jump of Ni^{2+} in the complex. The figure shows that there is no UV absorption at 400–800 nm for complexes II and III because the (n-1)d orbital of Zn^{2+} is in a full state and cannot undergo a d-d jump; thus, it is generally colourless or white, but complexes II and III are orange, which may be attributed to ionic polarization [28].

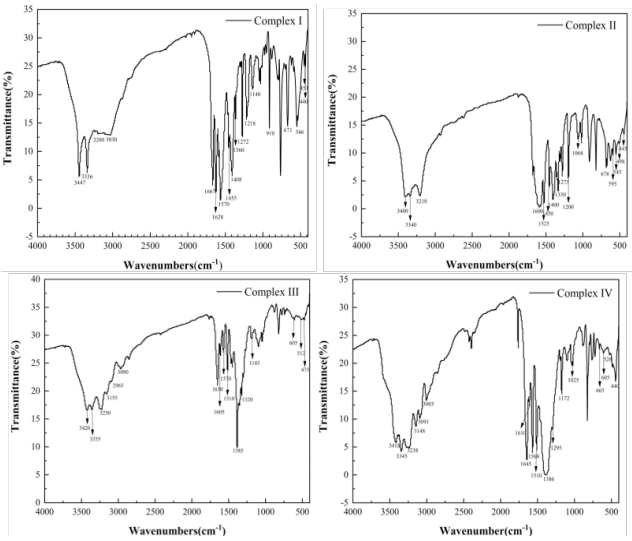

Figure 3: IR spectra of complexes (I)-(IV) in the range of 4000--400 cm^{-1}.

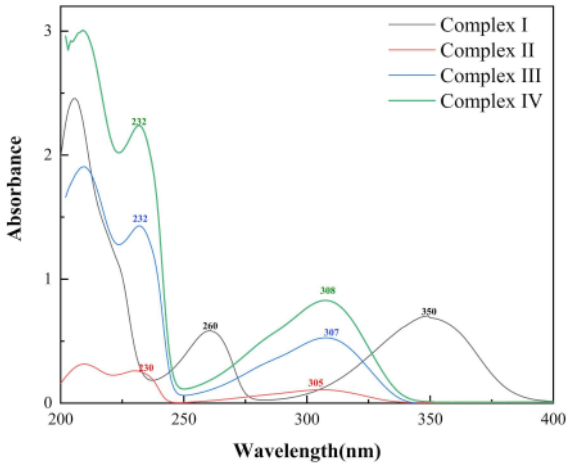

Figure 4: UV-visible spectra of complexes (I)-(IV).

Table 3: Cell inhibition rate of complexes I – IV.

Complex	Lung cancer A549		Liver cancer SMMC-7721		Lymphoma MDA-MB-231		Colon SW480	
	Cell inhibition							
	Average	SD	Average	SD	Average	SD	Average	SD
I	5.97	3.10	30.19	3.10	0.65	2.55	34.19	0.65
II	13.38	4.03	5.87	2.06	12.51	2.33	47.85	0.60
III	0.00	0.25	6.60	1.45	11.48	4.00	0.75	0.11
IV	11.03	1.84	17.28	0.67	21.96	1.69	18.68	0.38

Cytotoxicity assay of complexes (I)-(IV)

Table 3 shows the cellular inhibition of the four cancer cell lines via complexes (I)-(IV). The results indicate that the inhibitory effect of complex I on the hepatocellular carcinoma (SMMC-7221) cell line was significantly greater than that of complexes II and III, which may be related to the different ligands used. The ligands of complexes II and III were the same, but there was a significant difference in the inhibitory effect on the colon cancer (SW480) cell line, which might be related to the spatial geometrical configurations of the metal ions and the complexes. Metal complexes with octahedral configurations are more likely to interact with DNA and thus show better inhibitory effects than other spatial structures [29]. Our group will continue to work on this basis to synthesise complex crystals with better anticancer activity.

Conclusion

In this study, four novel complex structures were synthesized and characterized, and the inhibition rates of the complexes on four cancer cell lines were tested. The results showed that complex I and complex II inhibited SW480 colon cancer cells relatively well, but the overall effect was not satisfactory. Our group will continue research on this basis, hoping to synthesize metal complexes with better biological activities.

References

1. Han Y, Wen P, Li J, et al. Targeted Nano medicine in cisplatin-based cancer therapeutics [J]. Journal of Controlled Release. 2022, 345: 709-720.
2. Kaur M, Kumar S, Younis S A, et al. Post-Synthesis modification of metal-organic frameworks using Schiff base complexes for various catalytic applications [J]. Chemical Engineering Journal. 2021, 423: 130230.
3. Ramdass A, Sathish V, Babu E, et al. Recent developments on optical and electrochemical sensing of copper (II) ion based on transition metal complexes [J]. Coordination Chemistry Reviews. 2017; 343: 278-307.
4. Gasser G, Metzler-Nolte N. The potential of organometallic complexes in medicinal chemistry [J]. Current Opinion in Chemical Biology. 2012; 16(1-2): 84-91.
5. Bortolamiol E, Visentin F, Scattolin T. Recent advances in bio conjugated transition metal complexes for cancer therapy [J]. Applied Sciences. 2023; 13(9): 5561.
6. Riccardi C, Piccolo M. Metal-Based Complexes in Cancer [J]. International Journal of Molecular Sciences. 2023; 24(8): 7289.
7. Zhang H, Guo L, Tian Z, et al. Significant effects of counteranions on the anticancer activity of iridium(iii) complexes [J]. Chemical Communications. 2018; 54(35): 4421-4424.
8. Bhutani P, Joshi G, Raja N, et al. U.S. FDAApproved Drugs from 2015–June 2020: A Perspective [J]. Journal of Medicinal Chemistry. 2021; 64(5): 2339-2381.
9. Konakanchi R, Jyothi P, Kotha L R. Investigation of Structures, FTIR, FT-Raman, In Vivo Anti-Inflammatory, Molecular Docking and Molecular Characteristics of 2-Amino-3-Pyridine Carboxaldehyde and Its Copper (II) Complex Using Experimental and Theoretical Approach [J]. Polycyclic Aromatic Compounds, 2020: 123.
10. Wu Y, Wu T, Huang Y. A review: Biological activities of novel cyanopyridine derivatives [J]. Archive der Pharmazie. 2023.
11. Marinescu M, Popa C-V. Pyridine Compounds with Antimicrobial and Antiviral Activities [J]. International Journal of Molecular Sciences. 2022; 23(10): 5659.
12. Retnam C T G, Rose S V, Kumari B S. Synthesis, characterization, biological activity and molecular docking study of transition metal complexes from heterocyclic ligand system [J]. Journal of Molecular Structure. 2023; 1282: 135162.
13. Alshamrani M. Recent advances and therapeutic journey of pyridine-based Cu (II) complexes as potent anticancer agents: a review (2015-2022) [J]. Journal of Coordination Chemistry. 2023; 76(1): 1-19.
14. Zhang C, Xu C, Gao X, et al. Platinum-based drugs for cancer therapy and anti-tumor strategies [J]. Theranostics. 2022; 12(5): 2115-2132.
15. Konakanchi R, Rao K P, Reddy G N, et al. Zinc(II) complex: Spectroscopic, physicochemical calculations, anti-inflammatory and in silico molecular docking studies [J]. Journal of Molecular Structure. 2022; 1263: 133070.
16. Chasapis C T, Ntoupa P-S A, Spiliopoulou C A, et al. Recent aspects of the effects of zinc on human health [J]. Archives of Toxicology. 2020; 94(5): 1443-1460.
17. Huang L, He F, Wu B. Mechanism of effects of nickel or nickel compounds on intestinal mucosal barrier [J]. Chemosphere. 2022; 305: 135429.
18. Shakir M, Khanam S, Azam M, et al. Synthesis, Spectroscopic Characterization, and In Vitro Antimicrobial Screening of 16-Membered Tetraazamacrocyclic Schiff-Base Ligand and its Complexes with Co(II), Ni(II), Cu(II), and Zn(II) Ions [J]. Synthesis and Reactivity in Inorganic, Metal-Organic, and Nano-Metal Chemistry. 2011; 41(8): 979-986.
19. Hänsch R, Mendel R R. Physiological functions of mineral micronutrients (Cu, Zn, Mn, Fe, Ni, Mo, B, Cl) [J]. Current Opinion in Plant Biology. 2009; 12(3): 259-266.
20. Zhang L, Yin H, Zhang J-C, et al. Synthesis, crystal structure and anticancer activity of 4-chloro-2-methoxybenzoic acid transition metal complexes [J]. Journal of Molecular Structure. 2024; 1316: 139080.
21. EL Luttle, WJ Middleton, DD Coffman, VA Engelhardt, GN Sausen. J. Am. Chem. Soc. 1958; 80: 2832-2839.
22. AA Amer. J. Heterocyclic Chem. 2008; 55: 297-302.
23. IV Dyachenk, VD Dyachenko, PV Dorovatovsky, VN Khrustalev, VG Nenajdenko. Russ. J. Org. Chem. 2020; 56: 974-982.
24. Kumar A, Rai Y, Bhatt A N. Anti-cancer drug-mediated increase in mitochondrial mass limits the application of metabolic viability-based MTT assay in cytotoxicity screening [J]. Cytotechnology. 2024; 76(3): 301-311.
25. İlkimen H, Salün S G, Gülbandılar A, et al. The new salt of 2-amino-3-methylpyridine with dipicolinic acid and its metal complexes: Synthesis, characterization and antimicrobial activity studies [J]. Journal of Molecular Structure. 2022; 1270: 133961.
26. Raman N, Utthra P P, Chellapandi T. Insight into the in vitro anticancer screening, molecular docking and biological efficiency of

pyridine-based transition metal (II) complexes [J]. Journal of Coordination Chemistry. 2020; 73(1): 103-119.

27. Anjomshoa M, Fatemi S J, Torkzadeh-Mahani M, et al. DNA- and BSA-binding studies and anticancer activity against human breast cancer cells (MCF-7) of the zinc(II) complex coordinated by 5,6-diphenyl-3-(2-pyridyl)-1,2,4-triazine [J]. Spectrochimica Acta Part A: Molecular and Biomolecular Spectroscopy. 2014; 127: 511-520.

28. Hegde P L, Bhat S S, Revankar V K, et al. Syntheses, structural characterization and evaluation of the anti-tubercular activity of copper (II) complexes containing 3-methoxysalicylaldehyde-4-methylthiosemicarbazone [J]. Journal of Molecular Structure. 2022; 1257: 132589.

29. Abdolmaleki S, Khaksar S, Aliabadi A, et al. Cytotoxicity and mechanism of action of metal complexes: An overview [J]. Toxicology. 2023; 492: 153516.